Slow Cycle Fatigue Creep Performance of Pb-Free (LF) Solders

Vasu Vasudevan *, Xuejun Fan**, Tao Liu ***, and Dave Young *
Intel Corporation
*5200 Elam Young Pkwy, Hillsboro, OR 97124
*** 5000 Chandler Blvd, Chandler, AZ 85226
*** Dupont, WA,
Vasu.S.Vasudevan@Intel.com

Abstract

Electronics industry is successfully transitioning into Lead-Free (LF) solders to comply with government regulations. There are many challenges associated with reliability life prediction for LF solders such as the selection of temperature cycle test methods, material compatibility issues, and reliability models. This paper focuses on investigating the effect of extended dwell time on LF reliability under thermal cycling for both flip chip BGA packages and sockets. Extensive experimental temperature cycle results for different pitch FC BGAs, and sockets have shown that LF (Sn-4.0Ag-0.5Cu) solder has a better fatigue performance than Sn/Pb over a wide range of extended dwell times. Long-dwell time temperature cycle results revealed that LF will not cross over Sn/Pb performance in the extended dwell time testing up to 8-hour cycle time for the temperature range between -25 and + 100^0 C. It is also noted that the margin in fatigue life between LF and Sn/Pb becomes smaller with the increased dwell time. This is consistent with the creep properties of LF solder. Finite element modeling results corroborated the experimental data. Detailed failure analysis for both socket and flip chip BGA units demonstrated that LF has much less crack propagation rate than Sn/Pb even with very long dwell time showing better fatigue performance compared to Sn/Pb..

1. Introduction

With the world-wide electronic industry transition from the use of Sn/Pb eutectic solder to more environmental friendly lead-free (LF) solder composition, many manufacturing and reliability challenges were expected due to the difference in material and mechanical properties. Several lead-free solder alloy compositions have been studied to address issues including the increase of reflow temperature and material compatibility concerns such as tin whiskers, micro-voids for PCB Im/Ag coating and kirkendal type voids for PCB OSP coating. Tin–Silver–Copper (SAC) alloys are becoming the primary lead-free replacement for the eutectic Sn/Pb solder. Sn-3.0Ag-0.5Cu (SAC305) and Sn-4.0Ag-0.5Cu (SCA405) are most popular choices for the application demanding long-term reliability (fatigue life) and Sn-1.0Ag-0.5Cu (SAC105) alloy becomes the main choice for hand-held type application where drop performance is of primary importance.

In general, the published temperature cycling results showed that SAC solder is better in fatigue resistant than Sn/Pb eutectic solder. The fatigue life expectancy of LF solder was found to be 1.5 - 2.0X than that of Sn/Pb [1-5] solder. However, some experimental results showed the fatigue life of SAC is lower that Sn/Pb solder [6-7]. One key point to be noted from the published data is that the SAC alloy was only reported to have a lower fatigue performance under temperature cycle test condition when the peak cycle temperature was at or above 125^0C and the package construction provided little or no compliance (e.g., ceramic package type) in the solder joint interconnects. Another observation is that the reduction in fatigue performance of SAC solder due to longer dwell (soak) times appears to be higher than the reduction observed with Sn/Pb eutectic solder [6]. So, the long dwell time impact of SAC alloy has been raised as a concern and appropriate dwell time for SAC temperature cycling testing is a major controversy for product qualification. In the absence of industry-accepted SAC solder fatigue model, many believe that LF will show poor fatigue performance compared to Sn/Pb in temperature cycle testing with extended dwell time (typical of field conditions).

In this paper, we will report our extensive experimental results with extended dwell time under thermal cycling condition. Both flip chip BGA packages and socket BGA with enabling loads were tested at a wide range of dwell times under different configurations regarding board design and thermal solutions. The purpose of this paper is to review reliability results and also to understand the SAC reliability risk associated with long dwell time performance test.

2. Lead-Free Solder Materials, Process and Properties

The leading LF alloy choices are the near ternary eutectic Sn-Ag-Cu alloys. The ternary eutectic is close to Sn-3.5Ag-0.9Cu [8,9] with a melting temperature of 217˚C. The near eutectic, commercially available alloys are Sn-3.8Ag-0.7Cu and Sn-4.0Ag-0.5Cu compositions. The near ternary alloys yield three phases upon solidification: β-Sn, Ag_3Sn and Cu_6Sn_5 [9,10]. It has been reported that relatively large Ag_3Sn plates [8-10] can form during solidification of the near ternary eutectic Sn-Ag-Sn alloys. Moon et al. [8] have reported that Ag_3Sn plate nucleation and the ensuing growth occurs with minimal undercooling using the differential thermal analysis methods (DTA). The β-Sn phase requires significantly large undercooling to induce nucleation and thus final solidification. [10, 11]. Large Ag_3Sn plates can adversely affect the plastic deformation properties of the solders and cause plastic-strain localization at the boundary between the Ag_3Sn plates and the bounding β-Sn phase [12]. Frear et al. [13] have reported plastic strain localization at the boundary between the Ag_3Sn plates and the bounding β-Sn phase. The strain localization appears to be essentially grain boundary sliding, occurring at the boundary between these phases. The strain localization at the plate boundaries may be due to the coefficient of thermal expansion differences between the Ag_3Sn plates and the bounding β-Sn phase. In addition, the

plate orientation within the solder joint and its relation to the applied stress field are crucial in controlling the plastic deformation behavior and therefore in determining whether this phenomenon is important from a reliability standpoint. In the case of SAC405 sample, these plates are vertical and hence this phenomenon has been suppressed. To date, no early thermo-mechanical failures have been reported for SAC 405.

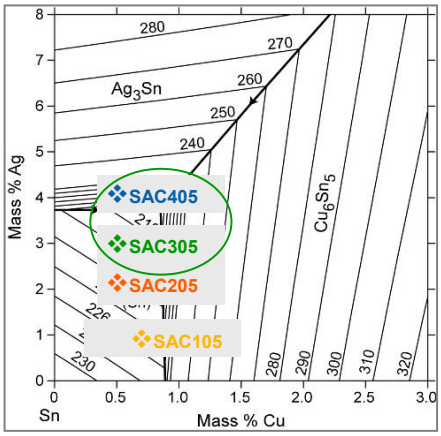

Figure 1:. The ternary Sn-Ag-Cu phase diagram.

Figure 1 shows thermodynamically calculated phase diagram in Sn-rich area along with experimentally-estimated ternary eutectic compositions by various companies and institutions (the thermodynamic calculation is based on Sn-3.38Ag-0.84Cu). Based on literature data, the possible eutectic composition lies between Sn-(3.2 to 4.7) wt. %Ag-(0.6 to 1.7) wt. %Cu. Sn-Ag-Cu alloy in this section will refer to eutectic or near eutectic Sn-Ag-Cu systems with eutectic melting temperature (Tm) of about 217ºC). The reference [12] has presented the temperature versus thermodynamically-obtained solid fraction of three SnAgCu solders and has proposed the melting or solidification sequence for these solders as follows. Sn-3.0Ag-0.5Cu solder, for example, is fully liquid above about 220ºC. On cooling, about 20 wt. % of molten solder is solidified into β-Sn (in other words, β-Sn is primary phase in Sn-3.0Ag-0.5Cu) at ~217ºC. On further cooling, remaining liquid is further solidified into Ag_3Sn and β-Sn (therefore, Ag_3Sn and β-Sn are proeutectic phases in this example) by the reaction: L-> Ag_3Sn +β-Sn. Finally, at ~216ºC, the remaining liquid is transformed into ternary eutectic phases (Ag3Sn, β-Sn and Cu_6Sn_5) by ternary eutectic reaction. Sn-3.5Ag-0.7Cu has Cu6Sn5 as primary phase and Ag_3Sn /Cu6Sn5 as proeutectic phases while Sn-3.9Ag-0.6Cu has Ag_3Sn and Ag_3Sn /β-Sn as primary and proeutectic phases, respectively. It is noted that Ag_3Sn intermetallic phase is a primary phase in Sn-3.9Ag-0.6Cu. Also, depending on the Ag content in the Sn-Ag-Cu alloy, it is found that this primary Ag_3Sn exists as large platelet while eutectic Ag_3Sn exists as fine fiber. The formation of large primary Ag_3Sn is shown to lead to reduced ductility in tensile testing and therefore can cause potential brittleness issue in the joint [12]. So, the microstructure can play a key role in LF alloy selection. Typically SAC 305 and SAC405 are recommended for longer fatigue life application where the IMC can reduce the fatigue crack propagation.

The melting points and mechanical properties of different solder alloy system are shown in Table 1. There is considerable variation in the published test data on mechanical properties of solder due to tolerances in the measurement equipment/techniques and variability in test specimen design and preparation. This has led to development of several constitutive material models for plasticity and steady state creep behavior of SAC solders. One difficulty has been the separation of time-independent (plastic) and time-dependent (creep) inelastic components from the measured strains. Wiese et al [14] studied the creep behavior of bulk, PCB sample, and Flip Chip solder joint samples of Sn4.0Ag0.5Cu solder and identified two mechanisms for steady state creep deformation for the bulk and PCB samples. They attributed these to climb controlled (low stress) and combined glide/climb (high stress) mechanisms and represented steady state creep behavior using a double power law model as shown below

$$\dot{\varepsilon} = \frac{\dot{\sigma}}{E} + A_1 D_1 \left(\frac{\sigma}{\sigma_n}\right)^3 + A_2 D_2 \left(\frac{\sigma}{\sigma_n}\right)^{12} \qquad (1)$$

where

$\dot{\varepsilon}$ = Total strain rate (1/sec)

σ = Stress (MPa)

E = Modulus of Elasticity (MPa) = $59533 - 66.667T$

T = Temperature (K)

$A_1 = 4.0 \times 10^{-7}$ 1/sec

$A_2 = 1.0 \times 10^{-12}$ 1/sec

$D_1 = \exp\left(\frac{-3223}{T}\right)$

$D_2 = \exp\left(\frac{-7348}{T}\right)$

σ_n = 1 MPa

The second term in the equation (1) represents the climb controlled creep strain and the third term represents the combined glide/climb strain. Figure 2 shows the creep strain rate as function of stress at different temperatures. As the stress increases, SAC shows steeper slope of strain rate vs. stress curve. Figure 2 also shows a comparison of creep behaviors of SACu and Sn/Pb. This figure clearly shows that at low stress levels, the steady state creep rate for SAC solder is two to four orders of magnitude lower than that for Sn/Pb solder for the same temperature. As the stress increases, SAC shows a steeper slope of strain rate vs. stress curve compared to Sn/Pb solder with cross-over points depending on the constitutive model and the temperature. This means that except at very high stresses, SAC is generally more creep resistant than Sn/Pb solder.

Table 1. Typical physical and mechanical properties of several solder alloys [13]

Solder	Melting Point (°C)	Young's Modulus (GPA)	Tensile Strength (MPa)	Creep strength in N/mm2 at 0.1 mm/min 20°C	199°C
Sn 37 Pb	183	39	40	3.3	1.0
Sn 3.5 Ag	221	51	58	13.7	5.0
Sn -3Ag-0.5 Cu	217-218	51	48	13	5.0
Sn-0.7Cu	227	59	32	8.6	2.1
Sn -3.8Ag-0.7Cu	217-218	51	58	13	5.5

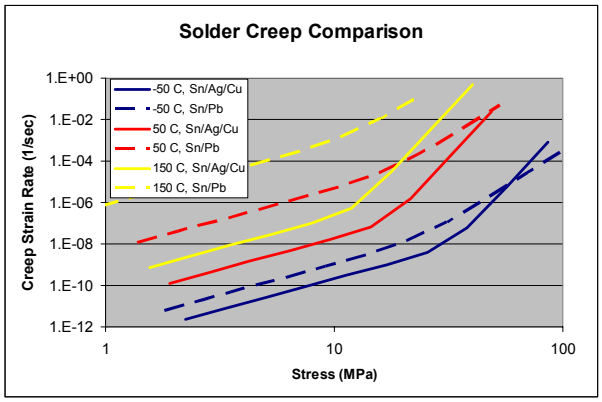

Figure 2: Sn/Pb vs. SAC 405 creep plots (ack: Pardeep Bhatti)

3. Experiment

3.1 Experimental Procedure

Air to Air temperature cycle testing was used to understand the solder fatigue life and solder joint reliability. Two types of thermal cycle chambers were used. One type is a conventional Ransco chamber with three shuttles and had a typical ramp rate of 15°C/min. Another type of chamber is single shuttle/zone chamber with slower ramp rate of about 3 to 5°C/min. Two different PCB test boards were used. One board was populated with multiple Flip Chip (FC) BGAs as shown in Figure 3. The other board design was a typical motherboard with sockets, BGAs and other components populated, which is called MTB. Such a MTB test board comes with thermal solutions for each component with enabling loads applied to the component, as shown in Figure 4.

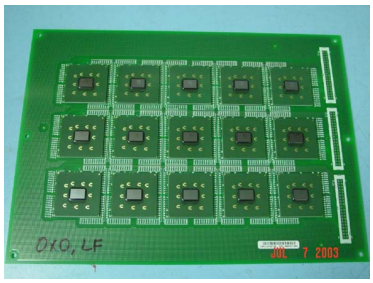

Figure 3: Multi-component FC BGA test board

Figure 4: MTB test board with sockets, FC BGA and simulated enabling loads on components of interest

For multi-component test, the FCBGA package and board attributes are listed in Table 2. The temperature cycle test conditions are given in Table 3, with three different dwell times and two temperature ranges. For MTB test, thermal cycle testing was performed with fully configured thermal solutions. Both sockets and FCBGAs were electrically monitored (in-situ) for different dwell time ranging from 20 minutes to 4 hours. The in-situ resistance behavior as a function of temperature cycle was compared for different dwell time. The in-situ resistance opens were correlated to solder joint cracks using dye and pull test and cross-section analysis. Two different FCBGA packages were assembled on the motherboard with heatsink applied. The package geometry is similar to the FCBGA package tested in the multi-component test. The socket with two different loading configurations was tested for both Sn/Pb and SAC405 solder alloys. Table 4 lists the testing conditions and sample sizes.

Table 2. FCBGA package and PCB board attributes for multi-component test board

Package attributes	
Package size	37.5 mmsq
Die size	11.7 X 9 mm
Solder ball dia	22 mil
Package Pad size	20 mil
Solder metallurgy	Eutectic (Sn/Pb 37) and Lead-free (95.5Sn4.0Ag0.5Cu)
Ball pitch	1 mm
Package surface finish	Electroless Nickel Immersion Gold
Substrate thickness	1.17 mm
Board attributes	
PCB Board size	10 X 10X 0.082 inch
Dielectric	Std FR4
PCB pad size	20 mil + - 2 mil
Stack up	6 layer board
PCB pad SF	HASL for Sn/Pb and Im/Ag for LF

Table 3. Temperature cycling conditions for multi-component board

Experiment Leg	Temperature cycle	Dwell (Soak)
1	-40°C to +85°C	15 min
2	-40°C to +85°C	30 min
3	-25°C to +125°C	90 min

Table 4. Temperature cycle conditions for MTB board

Test Vehicle	Cycle time	Solder Alloy	Ramp Rate ° C /Min
Enabling Design 1	1 hr	Sn/Pb	10-15
		LF	10-15
	4 hr	Sn/Pb	3-5
		LF	3-5
	8 hr	Sn/Pb	3-5
		LF	3-5
Enabling Design 2	1.5 hr	Sn/Pb	10-15
		LF	10-15
	4 hr	Sn/Pb	3-5
		LF	3-5
	8 hr	Sn/Pb	3-5
		LF	3-5

3.2. Experimental Results

FCBGA Reliability

Figure 5 gives the lognormal distribution plot for FC BGA package with two different dwell times of 15 minutes and 30 minutes, respectively. Temperature range of this test is -40°C to 85°C. It shows that the longer dwell time reduces the fatigue life significantly for both Sn/Pb and SnAgCu solders. However, Sn/Pb shows a smaller reduction compared to SnAgCu solder. It also shows that the gap in fatigue life between SnAgCu and Sn/Pb is reduced as dwell time is increased. Figure 6 shows 90-minute dwell time test data for the same package. Temperature range of this test is -25°C to 125°C. Although the gap of life between these two solders is smaller than with regular 15 minute dwell time, SAC showed better fatigue performance compared to Sn/Pb.

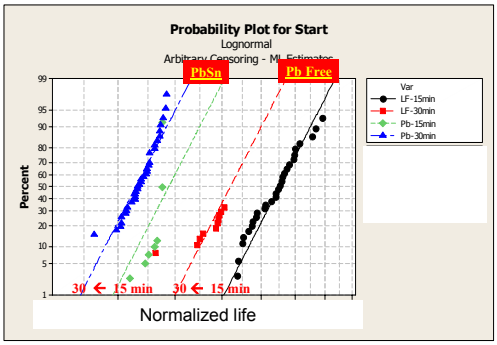

Figure 5: Lognormal plot for FCBGA package with two different dwell times (15-min and 30-min)

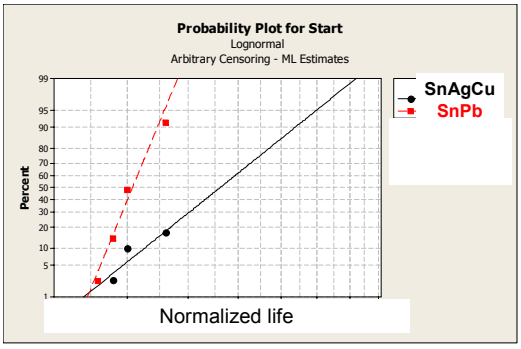

Figure 6: Sn/Pb vs. SnAgCu with 90 minute dwell time (temperature range: -25°C to +125°C)

For the extended 4-hour (240-min) dwell time temperature cycling test on MTB board, in-situ monitoring on FCBGA was stopped at 1000 cycles without any failures. Further, two FC BGA units were randomly picked at 1400 cycles from the Sn/Pb and SAC legs, respectively for cross-section failure analysis. As shown in Figure 7, the entire row of solder balls along the die edge were inspected using low magnification SEM.

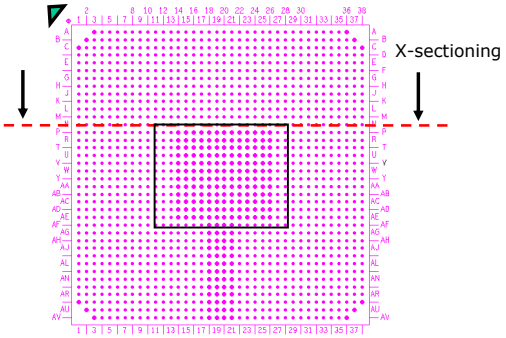

Figure 7: FCBGA solder ball layout and the location of cross-section (the center box denotes die area)

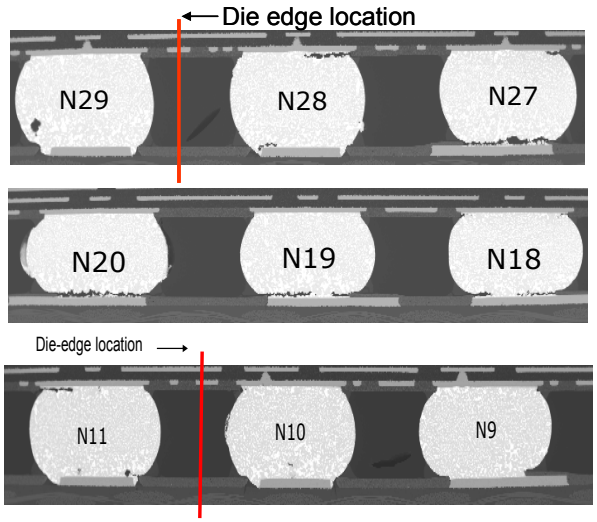

Figure 8: Low magnification SEM images of crack propagation of solder balls at die-edge for Sn/Pb unit after 1400 cycles with 4-hour dwell time

Figure 8 shows the low magnification SEM images of crack propagation for the selected solder balls under die shadow for the Sn/Pb unit. It indicates that several balls have complete cracks at the board side, and some partial cracks on the package side after 1400 cycles with 4-hour dwell time. The crack propagation is fatigue-type in bulk-solder material. Outside die shadow region, minimal crack propagation was observed. This is consistent with previous observations that the critical solder balls for FC BGA packages are always under die-shadow along die edge.

Figure 9 shows the low magnification SEM images of the crack propagation at the same locations as in Figure 8 but for the SAC unit. It can be seen that after 1400 cycles with 4-hour dwell time, the SAC unit has much less crack growth than that of the Sn/Pb unit. Again, the maximum crack growth occurs under die shadow region and the crack propagation is fatigue-type in bulk-solder material. This implies that the LF (SAC) alloy has better solder fatigue performance compared to Sn/Pb even with the extended dwell time of 4-hour for FC BGA packages.

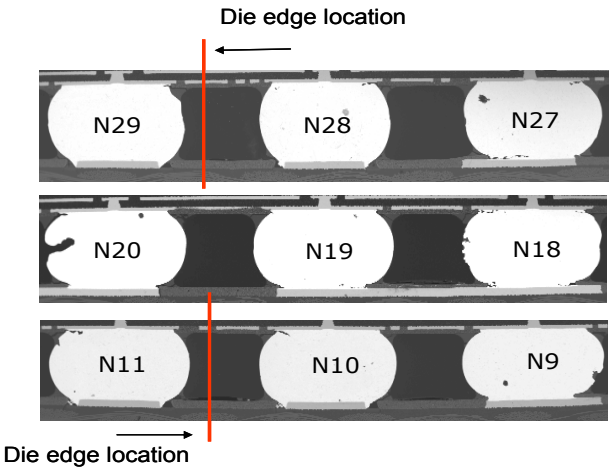

Figure 9: Low magnification SEM images of crack propagation of solder balls at die-edge for SAC unit after 1400 cycles with 4-hour dwell time.

Socket Reliability

Two different loading configurations of sockets were tested on MTB board. Figures 10, 11 and 12 plotted the lognormal distributions for the socket with different dwell times of 30, 120, and 240 minutes, respectively. Temperature range of this test is -25°C to 100°C.

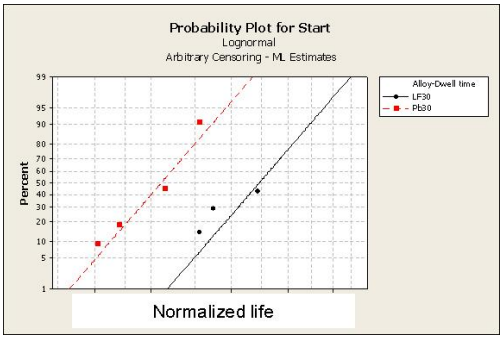

Figure 10: Lognormal plot for the socket with 30-minute dwell time (socket configuration 2 on MTB board)

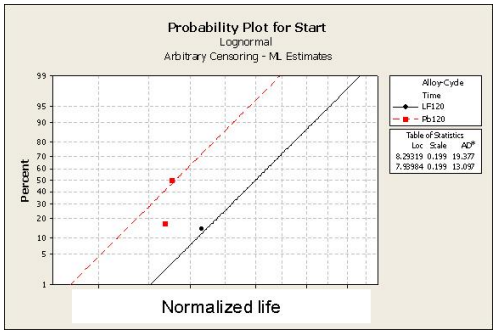

Figure 11: Lognormal plot for socket with 240-minute dwell time (socket configuration 2 on MTB board)

It was observed that the longer dwell time reduces the fatigue life significantly for both Sn/Pb and SAC solders (not shown in those figures with normalized plot). However, the LF (SAC) consistently performs better than Sn/Pb for each pair at different dwell times.

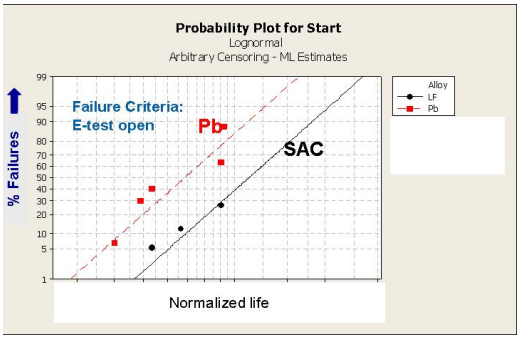

Figure 12: Lognormal plot for socket with 240-minute dwell time (socket configuration 1 on MTB board)

Two units were randomly picked at 1400 cycles with the 240-minute leg from both Sn/Pb and SAC units respectively, for cross-section failure analysis. As shown in Figure 13, the entire row of solder balls along the socket edge were inspected using low magnification SEM. Figure 14 shows the comparison of the typical images of the selected 3 balls for Sn/Pb and SAC units. It clearly indicates that the Sn/Pb has fatigue-type of crack on the board side and SAC unit is much more creep-resistant than Sn/Pb unit even after 1400 cycles with 480-min cycle time.

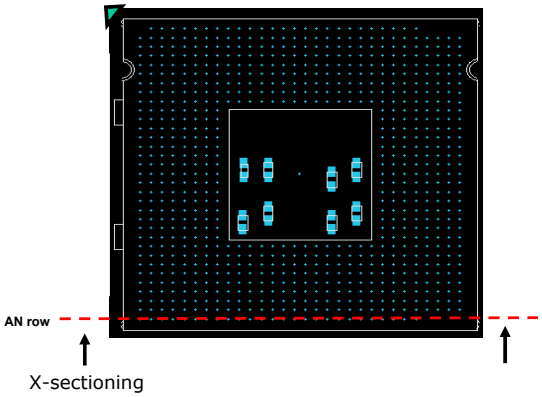

Figure 13. Socket solder ball layout and indentification of cross-section location

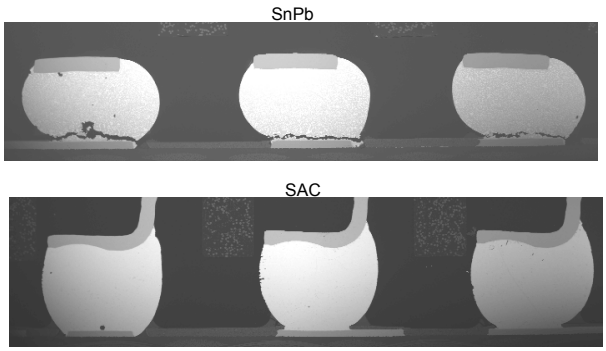

Figure 14 : Cross-section analysis for the socket units with the extended dwell time of 240-minute under -25°C to 100°C temperature cycling condition.

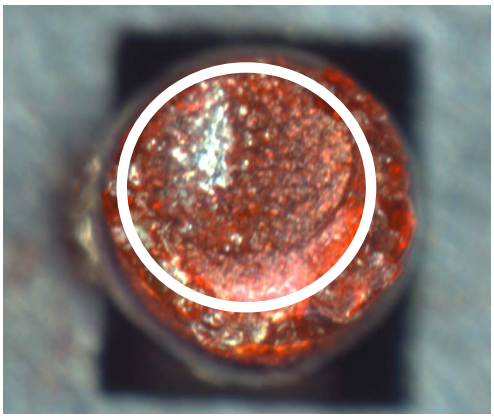

Figure 15a: Dye penetration results of socket after 1900 cycles (240 min cycle time) for Sn/Pb solder showing 90% crack

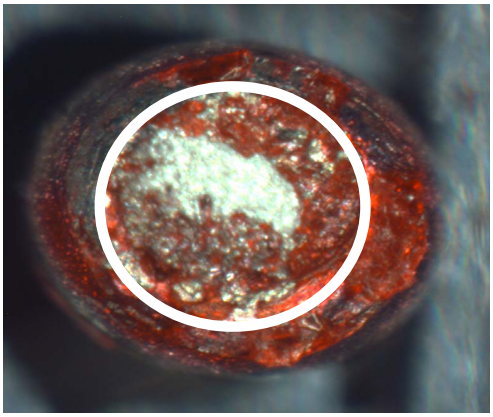

Figure 15b: Dye penetration results of socket after 1900 cycles (240 min cycle time) for LF solder showing 60% crack

Figure 15 shows the comparison of post temp cycle solder crack area between Sn/Pb and LF solder showing LF solder has less solder crack area for 240 min cycle time test. The lesser solder crack area observed for the LF samples post temp cycle test show higher fatigue resistance for LF. Figure 16 plotted the lognormal distributions for three different dwell times, i.e., 30-min, 120-min and 240-min respectively for SAC socket. It is unexpected to see that 30-min dwell time results in shorter life than 240-min. It is noted from the Table 4 that the 30-min dwell time leg used the two-zone chamber with a ramp rate at 15°C per minute, while 120-min and 240-min legs used a single-zone chamber at 5°C per minute ramp rate. It appears that the ramp rate plays a significant role in fatigue life. With faster ramp rate, more damage could be induced at ramp period, which might be more severe than the damage induced with the extended dwell time of 120-minute.

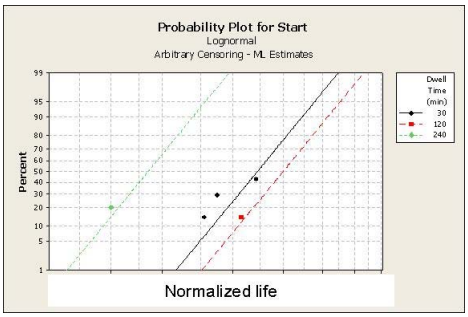

Figure 16: Lognoraml plots for SAC socket with different dwell times and ramp rates (120-min and 240-min legs have slower ramp rate than 30-min leg)

4. Finite Element Analysis

Finite element analysis was performed to investigate the concern of lead-free solder joint reliability with long dwell times. A full non-linear, quarter symmetry finite element model was created for FC BGA packages. The details of finite element model are described in ref. [15-16]. The creep model given by Equation (1) is used to evaluate the creep accumulation during thermal cycling. Figure 17 and Figure 18 show the per-cycle total accumulated creep strain for Sn/Pb and SAC respectively. Four different dwell times were considered: 15 min, 30 min, 90 min, and 480 min (8hours). Figure 16 shows that for SAC, the total per-cycle creep strain with 8-hour dwell time is ~4X the value with 15 minute dwell time. However, from Figure 18, Sn/Pb shows only ~2X increase over the same range. This implies that since SAC creeps more slowly than Sn/Pb, SAC will continue to creep with longer dwell time. And since Sn/Pb creeps faster, majority of stress relaxation is already complete in 15 minutes with little additional creep accumulation beyond that. These results corroborate the experimental data.

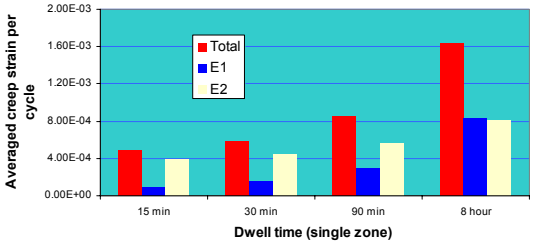

Figure 17: Average creep strain on package side for SAC solder

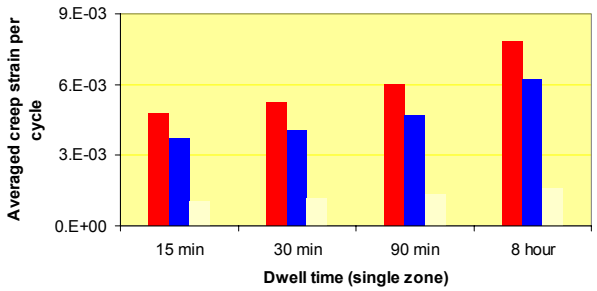

Figure 18: Average creep strain on package side for Sn/Pb solder

Figures 19 and 20 show the accumulated creep strain history with time in the first three cycles for Sn/Pb and SAC, respectively. These graphs show that total creep strain for 15 minutes is much lower than with 8 hour dwell time. Figure 18 shows that for SAC, creep accumulation at low temperature dwell and high temperature dwell is still continuing and no asymptote is evident even at 8 hour dwell time. Figure 20 shows that for Sn/Pb, the stress is completely relaxed at high temperature for Sn/Pb, thus no further creep is accumulated at high temperature dwell. However, due to high stress at low temperature, it is not fully relaxed, and the creep accumulation is still on going after 8-hour dwell time for Sn/Pb.

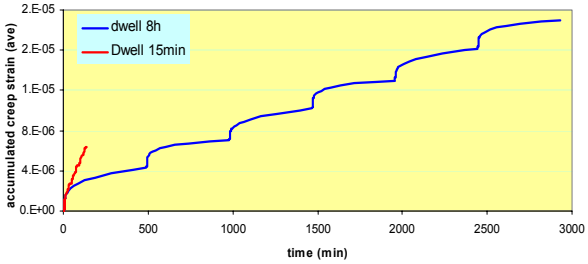

Figure 19: Accumulated creep strain history for SAC

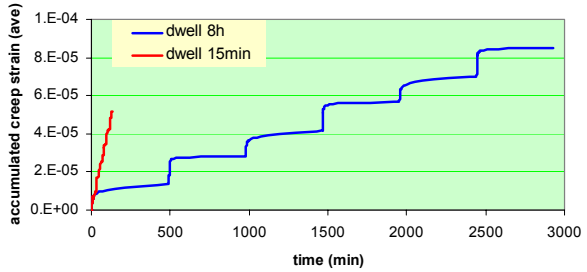

Figure 20: Accumulated creep strain history for Sn/Pb

5. Discussions

5.1. Dwell Time Effect

Long dwell time temperature cycle results revealed that the SAC405 will not cross over Sn/Pb performance in the extended dwell time testing up to 8-hour cycle time for the temperature range between -25 and + 100^0 C for both FC BGA packages and sockets. SAC405 solder has a better fatigue performance than Sn/Pb over a wide range of the extended dwell time. However, above test results did indicate that the margin in fatigue life for SAC over Sn/Pb is reduced with the increased dwell time. This is consistent with the SAC creep properties and finite element modeling results. Assuming that $t_1<t_2$, where t_1 and t_2 are two different dwell times, the characteristic lives can be denoted as $N_1^{SAC} > N_2^{SAC}$, and $N_1^{Sn/Pb} > N_2^{Sn/Pb}$, respectively for SAC and Sn/Pb. If the power law between the fatigue life and dwell time is assumed, i.e.,

$$(N_1^{SAC}/ N_2^{SAC}) = (t_1/t_2)^{-a\_SAC} \quad (2)$$

$$(N_1^{Sn/Pb}/ N_2^{Sn/Pb}) = (t_1/t_2)^{-a\_Sn/Pb} \quad (3)$$

where a_SAC and a_Sn/Pb are acceleration factors for SAC and Sn/Pb, respectively with respect to dwell time. Since SAC creeps more slowly than Sn/Pb, SAC will continue to creep with longer dwell time. And since Sn/Pb creeps faster, majority of stress relaxation is almost complete at the earlier time, we expect,

$$N_1^{SAC}/ N_1^{Sn/Pb} > N_2^{SAC}/ N_2^{Sn/Pb} \quad (4)$$

Based on Equations (2) to (4), we can obtain

$$a\_SAC > a\_Sn/Pb \quad (5)$$

which means that SAC has greater acceleration factor and better fatigue performance than Sn/Pb. Such a relationship is consistent with the experimental data shown in Figures 5-6, and 10-12. However, it is not known that whether a single acceleration factor in power law formulation could describe accurately the dwell time dependency.

Based on the experimental data shown above, it appears that it might not be necessary to change the dwell time from the current 15min dwell time to 30min dwell time. The change of dwell time to 30min will significantly increase the cycle time of test, but the similar trend is expected with regard to the 15 minute dwell time.

Finite element modeling results show that creep accumulation not only is induced at high temperature dwell, but at low temperature dwell as well. It is necessary to separate the effect of dwell time at high-extreme temperature and low-extreme temperature. This will be our future study.

5.2. Ramp Rate Effect

From Figure 16, it appears that the ramp rate plays a significant role in fatigue life. With faster ramp rate, more damage could be induced at ramp period, which might be more severe than the damage induced with the extended dwell time. Our previous study results [17] also showed that the lead-free solder joint during thermal shock fails faster than thermal cycling. The faster ramp rate does impose more damage on solder joint than a slow ramp rate. These results are consistent with the tests reported in ref. [18-19]. However, based on the creep model in equation (1), we were not able to describe the ramp rate effect. This suggests that it is necessary to investigate the creep material properties with regard to different ramp rate to understand the failure mechanism.

5.3. Tmax Effect

Tmax denotes the high dwell temperature in thermal cycle test Several studies have shown that the SAC alloy has a lower fatigue performance under temperature cycle test

condition when the peak cycle temperature was at or above 125^0C and the package construction provided little or no compliance (e.g., ceramic package type) in the solder joint interconnects. Our test result in Figure 6 seems to indicate that Tmax plays a significant role in SAC solder fatigue life. This suggests that the accelerated temperature cycle test for LF solder should be performed below 0.8 melting temperature in Kelvin (TM). Syed etal [7] observed this behavior for ceramic package and Osterman et al [20] highlighted this behavior for LCC packages. More future work is needed to explain this behavior for LF solder and understand failure mechanism change if any for temperatures above 0.8 TM. The proposed temp cycle conditions for LF solder is shown in figure 21. The temp cycle results to date show that LF solder show higher fatigue perfotmance when the ramp rate is below <15 ^{o} C/min and Tmax below 125 ^{o} C

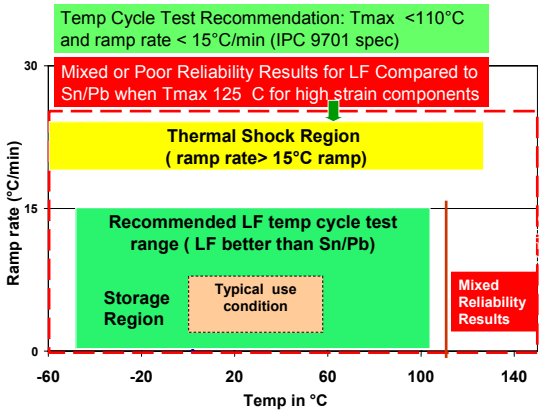

Figure 21: Proposed temp cycle test conditions for LF solder

Conclusion

Based on the extensive temperature cycling test results for both flip chip BGAs and sockets, it is clear that the SAC (Sn-4.0Ag-0.5Cu) consistently performs better than Sn/Pb under various dwell time conditions and different ramp rates. Detailed failure analysis on long-dwell time samples confirmed that the SAC has much less crack fatigue-propagation rate than Sn/Pb even with 8-hour per-cycle time TC test with a temperature range from -25 and + 100^0 C. In conclusion, LF (SAC) solder showed better fatigue performance compared to Sn/Pb solder.

Acknowledgments

The authors would like to acknowledge the following Intel employees Pardeep Bhatti, Don Woomer, Gerry McCauley, Satish Parupalli, Jim Maguire, Satyajit Walwadkar, Phil Butler, Hyunchul Kim and Deepak Goyal for their contributions and support towards this study

References

1. J.-P. Clech, in Proc IPC/SMEMA Council APEX 2004 Conf (Anaheim, CA, Feb. 23–26, 2004), pp. S28-3-1–S28-3–14
2. P. Roubaud, G. Henshall, R. Bulwith, S. Prasad, F. Carson,S. Kamath, E. O'Keeffe, in SMTA International Proceedingsof the Technical Program (Edina, MN, 2001) pp. 803–809
3. M. Meilunas, A. Primavera, S. Dunford, in Proc. of the IPCAnnual Meeting (New Orleans, LA, Nov. 3–7, 2002) pp. S08-5–1 to S08-5–14
4. G. Swan, et al. Proc IPC/SMEMA Council APEX 2001 Conf(San Diego, CA, Jan. 14–18, 2001) pp. LF2-6-1–LF2-6
5. D. Nelson, H. Pallavicini, Q. Zhang, P. Friesen, A. Dasgupta,J SMT 17(1), 17 (2004)
6. J. Bartelo, et al., in Proc IPC/SMEMA Council APEX 2001Conf (San Diego, CA, Jan. 14–18, 2001), pp. LF2-2-1–LF2-2-12
7. A. Syed, in Proc. International Symposium on Advanced Packaging Materials Processes, Properties and Interfaces(Piscataway, NJ, 2001) pp. 143–147
8. Moon, K. W., Boettinger, W. J., Kitten, U. R., Biancaniello, F. S. and Handwerker, C. A., J. Electron. Mater., 29, 1122 (2000).
9. Loomans, M. E. and Fine, M. E., Metall. Mater. Trans. A, Phys. Metall. Mater. Sci., 31A, 1155 (2000).
10. Jeng, K. and Tu, K.N., Mater. Sci. Engg. R38, 2002, 55.
11. NISTDocument www.metallurgy.nist.gov/phase/solder/agcusn.html.
12. Ohnuma, I., Miyashita, M., Anzai, K., Liu, X.J., Ohtani, H., Kainuma, R. and Ishida, K., J. Electron. Mater., 29, 1137, 2000.
13. Frear, D. R., Jang, J.W., Lin, J. K., and Zhang, C., JOM, 53(6), 28, 2001.
14. Wiese, Steffen; Meusel, Ekkehard; Wolter, Klaus-Juergen, Microstructural dependence of constitutive properties of eutectic Sn-Ag and Sn-Ag-Cu solders, Proceedings - Electronic Components and Technology Conference, 2003, p 197-206
15. Xuejun Fan, Min Pei, and Pardeep K. Bhatti, Effect of Finite Element Modeling Techniques on Solder Joint Fatigue Life Prediction of Flip-Chip BGA Packages, ECTC 2006
16. Min Pei; Xuejun Fan; and Pardeep K. Bhatti, Field condition reliability assessment for Sn/Pb and SnAgCu solder joints in power cycling including mini cycles, IEEE Electronic Components and Technology Conference (ECTC), 2006, May 30 - June 2, San Diego, CA
17. Fan, X., Rasier, G., Vasudevan, V.S., "Effects of Dwell Time and Ramp Rate on LeadFree Solder Joints in FCBGA Packages Electronic Components and Technology", ECTC 2005. pp. 901 - 906
18. Zhai, C., Sidharth, and Blish, R., "Board Level Solder Reliability Versus Ramp Rate and Dwell Time During Temperature Cycling," IEEE Transactions On Device Reliability and Material Reliability, Vol. 3, No. 4, December 2003. pp. 207-212.
19. Shubhada Sahasrabudhe, Eric Monroe, Shalabh Tandon, Mitesh Patel, "Understanding the Effect of Dwell Time on Fatigue Life of Packages Using Thermal Shock and Intrinsic Material Behavior", ECTC 2003
20. Michael Osterman and Abhijit Dasgupta, "Life expectancies of Pb-free SAC solder interconnects in electronic hardware' J Mater Sci: Mater Electron (2007) 18: pp229–236